Soft Matter

PAPER

Structural and microscopic relaxations in a colloidal glass

Flavio Augusto de Melo Marques,*[a] Roberta Angelini,[bc] Emanuela Zaccarelli,[cd] Bela Farago,[e] Beatrice Ruta,[f] Giancarlo Ruocco[ac] and Barbara Ruzicka[bc]

The aging dynamics of a colloidal glass has been studied by multiangle dynamic light scattering, neutron spin echo, X-ray photon correlation spectroscopy and molecular dynamics simulations. The two relaxation processes, microscopic (fast) and structural (slow), have been investigated in an unprecedentedly wide range of time and length scales covering both ergodic and nonergodic regimes. The microscopic relaxation time remains diffusive at all length scales across the glass transition scaling with wavevector Q as Q^{-2}. The length-scale dependence of structural relaxation time changes from diffusive, characterized by a Q^{-2}-dependence in the early stages of aging, to a Q^{-1}-dependence in the full aging regime which marks a discontinuous hopping dynamics. Both regimes are associated with a stretched behaviour of the correlation functions. We expect these findings to provide a general description of both relaxations across the glass transition.

1 Introduction

The dynamical behaviour of glass-forming systems has long been the subject of intense research.[1] One important feature of disordered systems is that the dynamics of density fluctuations is characterized by a two-step decay, which implies the presence of two main relaxation processes:[2] a microscopic or fast relaxation, associated with the interactions between a particle and the cage of its nearest neighbors followed by a structural or slow relaxation process, related to the structural rearrangements of the particles. These two distinct processes have been observed in simple monatomic liquids,[3] hydrogen bonded liquids,[4,5] structural glasses,[6–8] colloids[9–11] and DNA nanostars.[12] Furthermore Mode Coupling Theory (MCT)[13] has predicted the evolution of the two relaxations when a system goes from the liquid to the arrested state: this may happen *e.g.* by changing the temperature, packing fraction or waiting time (aging). However, even if the supercooled liquid phase above T_g in glass forming materials has been widely investigated with both DLS[7,14] and neutron scattering techniques,[15–19] it is still not clear how the two relaxation processes behave at the liquid–glass transition. While in a liquid the dynamics is known to be diffusive, a

change in particle dynamics should occur, as found in numerical simulations,[20,21] from diffusive to activated in the glass. The signature of this change at different length scales can be revealed by investigating the wavevector Q dependence of the relaxation times. Several numerical studies on different systems such as water,[22] *ortho*-terphenyl[23] and hard spheres[24] reported a subquadratic dependence of the structural relaxation time approaching the glass state. A recent theoretical work based on activated MCT has rationalised these findings providing a microscopic explanation for the change of dynamics across the glass transition.[25] So far, there has been no clear experimental proof of this scenario due to technical difficulties. Moreover, a full description encompassing both relaxation processes and their behaviour at different length scales is missing.

This is the aim of the present work where the aging investigation of a colloidal system makes possible a detailed study across the glass transition. In particular the waiting time t_w and wavenumber Q dependence of both fast $\tau_1(Q)$ and slow $\tau_2(Q)$ relaxation times is monitored through a combination of multiangle Dynamic Light Scattering (DLS), Neutron Spin Echo (NSE), X-ray Photon Correlation Spectroscopy (XPCS) and Molecular Dynamics (MD) simulations. In this way we access an unprecedentedly wide range of time and length scales and we find a different behaviour for the two relaxations across the glass transition. While the microscopic one remains unperturbed, indicating an unchanged, diffusive single particle dynamics at short times, the structural relaxation shows a clear change. Indeed, τ_2 going from the liquid to the arrested state undergoes a transition from a Q^{-2} to a Q^{-1} behaviour. Previous studies in aqueous Laponite dispersions[11,26] reported a Q^{-2} dependence for both microscopic and structural relaxation

[a]Center for Life Nano Science, IIT@Sapienza, Istituto Italiano di Tecnologia, Viale Regina Elena 291, I-00161 Roma, Italy. E-mail: flavio.marques@iit.it; Tel: +39 06 4991 3505

[b]IPCF-CNR, I-00185 Roma, Italy

[c]Dipartimento di Fisica, Sapienza Università di Roma, Piazzale Aldo Moro 5, I-00185, Italy

[d]ISC-CNR, I-00185 Roma, Italy

[e]Institute Laue-Langevin, BP 156, F-38042 Grenoble, France

[f]European Synchrotron Radiation Facility, B.P. 220 F-38043 Grenoble Cedex, France

times in the ergodic DLS regime. Later on studies on different systems *e.g.* colloids,[27,28] clays,[29–32] metallic glasses,[33] polymers,[34–36] and supercooled liquids[37] reported a Q^{-1} dependence of the structural relaxation time associated with an anomalous compressed exponential relaxation of the correlation functions attributed to hyperdiffusive dynamics.[38] Differently, in the present study the relaxation curves at long times are always described by a stretched exponential, which allow us to interpret the crossover from a Q^{-2} behavior to a Q^{-1} behavior across the glass transition as a signature of a change from diffusive dynamics to discontinuous hopping of caged particles, as predicted in ref. 25.

2 Materials and methods

We used a widely studied colloidal clay,[39–45] Laponite RD dispersions, prepared using the same protocol described in ref. 45. When dispersed in water Laponite develops a charged colloidal suspension of disks of 25 nm diameter and 0.9 nm thickness. All measurements have been performed using D_2O (EURISO-TOP) of purity ≥99.9% as a solvent. As recently shown the H/D isotopic substitution, required to gain contrast in neutron scattering measurements, does not qualitatively affect the aging behaviour of Laponite.[46] The waiting time origin ($t_w = 0$) is the time at which the dispersion is filtered directly in glass tubes with a diameter of 10 mm for DLS and of 2 mm for XPCS and in quartz cells with dimensions of 30 mm × 40 mm × 4 mm for NSE measurements. To avoid CO_2 degradation all samples were prepared and sealed inside a glovebox under a nitrogen atmosphere. All experiments were performed at the same molar concentration of a $C_w = 3.0\%$ sample in salt free water. At this weight concentration the system forms a Wigner glass[26,47] due to repulsive electrostatic interactions. This is a glass occurring in a dilute system which shares the main features of denser glasses, including a two-step decay.[48–50]

DLS measurements were performed with a multi-angle setup in the time range between 10^{-6} s and 1 s. A solid state laser with a wavelength of 642 nm and a power of 100 mW and single mode collecting fibers at five different scattering angles are used. Time autocorrelation functions are therefore simultaneously acquired at wavenumbers $Q = 6.2 \times 10^{-4}$, 1.1×10^{-3}, 1.5×10^{-3}, 1.8×10^{-3} and 2.1×10^{-3} Å^{-1} by calculating the intensity autocorrelation function as $g_2(Q,t) = \frac{\langle I(Q,t_0)I(Q,t_0+t)\rangle}{\langle I(Q,t_0)\rangle^2}$ where $\langle\dots\rangle$ denotes the temporal average over t_0. DLS is used only when the system is ergodic in the early aging, also referred to as cage forming, regime characterized by a structural relaxation time with a waiting time exponential dependence $\tau_2(t_w) \propto e^{t_w}$.[41]

XPCS measurements were performed at the ID10 beamline at the European Synchrotron Radiation Facility (ESRF, Grenoble, France) in a Q-range between 3.1×10^{-3} and 2.2×10^{-2} Å^{-1} including the peak of the static structure factor occurring at $Q_{peak} \sim 1.6 \times 10^{-2}$ Å^{-1} as in the H_2O solvent.[47] Using an incident partially coherent X-ray beam with energy fixed at 8 keV a series of scattering images were recorded by using a charged coupled

device (CCD) and the ensemble averaged intensity autocorrelation function $g_2(Q, t)$ was calculated by using a standard multi tau algorithm after having ensemble averaged over the detector pixels mapping onto a single Q value.[51] XPCS can thus be used when the system is non-ergodic in the full aging regime characterized by a waiting time power law dependence of the structural relaxation time $\tau_2(t_w) \propto t_w^\alpha$ with $\alpha \sim 1$.[41]

NSE measurements were performed at the spectrometer IN15 of the Institute Laue-Langevin (ILL, Grenoble, France) at larger wavevectors ($1.3 \times 10^{-2} < Q < 1.3 \times 10^{-1}$ Å^{-1}) and at shorter relaxation times (up to 2×10^{-7} s) with respect to DLS and XPCS. We used wavelengths of 10, 16 and 22.8 Å yielding time ranges (0.35–50) ns, (1.4–206) ns and (4.1–598) ns, respectively. While DLS and XPCS measure the normalized intensity correlation function $g_2(Q, t) = 1 + b[g_1(Q, t)]^2$ (Siegert relation), respectively through temporal averages (ergodic regime) and ensemble averages (non-ergodic regime), NSE directly accesses the intermediate scattering function $g_1(Q, t)^2$.

We complemented the experimental measurements with MD simulations for a simple model of low-density glass-former, *i.e.* a 50–50 non-crystallising binary mixture of $N = 1000$ Yukawa particles of equal screening length ξ and different repulsion strengths.[49]† The system was found[49] to undergo a Wigner glass transition upon decreasing temperature T. To mimic the experimental situation, we performed a quench inside the glassy region at a fixed number density $\rho = 0.002984$. The system was equilibrated at high $T = 1.0 \times 10^{-3}$ and then instantaneously quenched to $T = 1.6 \times 10^{-5}$, below the glass transition occurring at $T_g \sim 1.7 \times 10^{-5}$. The waiting time origin was the time of the quench. Self intermediate scattering functions $F^s(Q, t)$ have been calculated for different wave vectors as a function of waiting time, averaging over 20 independent quenches to improve statistics.

3 Results

Fig. 1(a) shows the normalized intensity correlation functions measured by using DLS at initial waiting time ($t_w = 9$ min) for different Q-values (symbols) and the corresponding fits (full lines) obtained through a typical double exponential decay:

$$g_2(q,t) - 1 = b\left[a e^{-\left(\frac{t}{\tau_1}\right)^\gamma} + (1-a)e^{-\left(\frac{t}{\tau_2}\right)^\beta} \right]^2 \quad (1)$$

where the parameters a and $(1 - a)$ are the amplitudes of the two relaxation modes, b is the coherence factor, τ_1 is the fast relaxation time connected to the microscopic motion of particles, τ_2 is the slow relaxation time related to the structural rearrangement, and γ (here $\gamma = 1$ (ref. 11 and 52)) and β measure the distribution widths of the two relaxations.

The Q-dependence of the fast and slow relaxation times is reported in Fig. 1(b) at different waiting times. While τ_1 shows a moderate waiting time dependence, τ_2 increases significantly

---

† Lengths and times are measured in units of ξ and $\xi/(m\varepsilon)^{1/2}$ respectively, where m is the mass of the particles and ε is the unit of energy. Temperature is measured in units of ε (*i.e.* $k_B = 1$ where k_B is the Boltzmann constant).
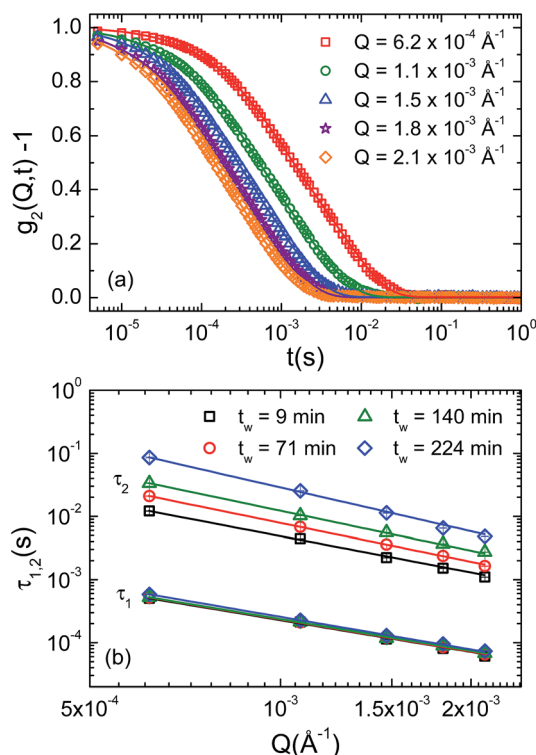
Fig. 1 (a) Normalized intensity correlation functions measured using DLS for different Q-values at $t_w = 9$ min. The solid lines are the fits obtained through eqn (1) with $\gamma = 1$. (b) Q-dependence of the fast τ_1 and slow τ_2 relaxation times at different waiting times. The solid lines are power law fits of the data as $\sim Q^{-n}$ where $n = 1.70 \pm 0.06$ for τ_1 and $n = 2.02 \pm 0.19$ for τ_2.
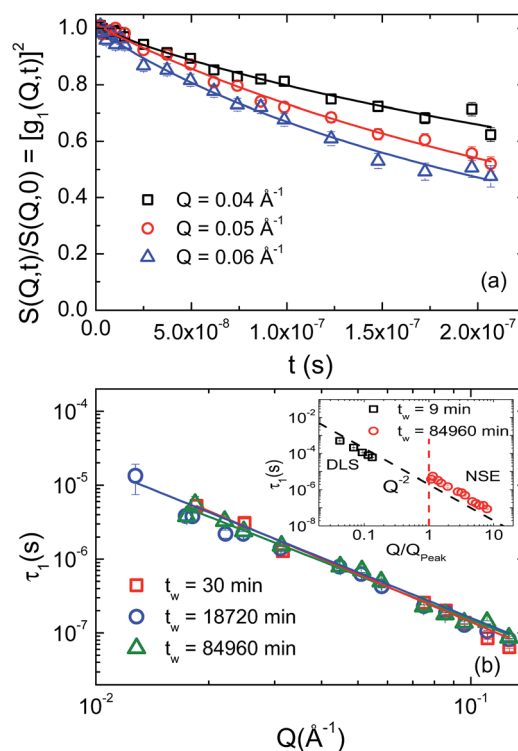

Fig. 2 (a) Dynamic structure factor obtained from NSE measurements for different Q-values at $t_w = 30$ min. The solid lines are stretched exponential fits with $\beta \sim 1$. (b) Q-dependence of the fast relaxation time at different waiting times. The solid lines are power law fits of the data as $\sim Q^{-n}$ where $n = 1.97 \pm 0.24$. Inset: comparison between fast relaxation times measured using DLS ($t_w = 9$ min) and NSE ($t_w = 84\,960$ min) as a function of Q/Q_{peak}. The dashed line indicates the Q^{-2} behaviour. The red vertical line indicates the position of the structure factor peak.

with t_w. Both times are well described by power law fits $\sim Q^{-n}$ with $n \sim 2$ (solid lines in Fig. 1(b)). Hence both microscopic and structural relaxation times display an almost quadratic wave vector dependence in the DLS (early aging) regime, which is the signature of diffusive dynamics for both relaxations at these early waiting times. These findings are in agreement with previous studies on Laponite water suspensions.[11,26,31,32]

Fig. 2(a) shows the dynamic structure factors measured by using NSE at different wavevectors (symbols) together with single stretched exponential fits (full lines). The corresponding fast relaxation times are shown in Fig. 2(b). We find that τ_1 scales as $\sim Q^{-2}$ during the whole experiment. As reported in the inset of Fig. 2(b) the estimate of τ_1 obtained from the NSE fits is in good agreement with that obtained by DLS, taking into account the large difference in Q between these techniques. Since the studied sample experiences a sol to Wigner glass transition at $t_w \approx 600$ min (derived as in ref. 52), NSE results ensure that the microscopic relaxation time remarkably scales as Q^{-2} both in the early aging and full aging regimes indicating that the short-time dynamics remains diffusive for all the investigated dynamical ranges even in the arrested state.

In Fig. 3(a) normalized intensity correlation functions probed by using XPCS in the full aging regime are shown at different Q-values (symbols). At these long waiting times the fast relaxation time τ_1 is out of the XPCS detection window. Hence

only the slow relaxation time τ_2 can be measured and only the second term of eqn (1) is used to fit the data (full lines in Fig. 3(a)). We notice that in our case DLS measurements allow to probe relaxation times up to $\sim 10^{-1}$ s (higher limit in Fig. 1(b)), reached for the sample in the ergodic region at waiting time $t_w = 224$ min, while XPCS measurements permit to access relaxation times above $\sim 10^2$ s (lower limit in Fig. 3(b)) achieved for the sample in the non-ergodic region at waiting time $t_w = 743$ min. Fig. 3(b) shows the Q-dependence of τ_2 at different waiting times (symbols) and the associated power law fits (full lines) as $\sim Q^{-n}$. In this regime we find $n \simeq 1$ ruling out the diffusive dynamics. Therefore a crossover from the DLS early aging regime characterized by $\tau_2(Q) \propto Q^{-2}$ to the XPCS full aging regime characterized by $\tau_2(Q) \propto Q^{-1}$ is observed. As shown in Fig. 4 this crossover is also associated with a typical dual waiting time dependence of the structural relaxation time with $\tau_2(t_w) \propto e^{t_w}$ at short waiting times probed by DLS and $\tau_2(t_w) \propto t_w^{\alpha}$ with $\alpha \sim 1$ at long waiting times probed by XPCS. In both cases the intensity correlation functions are described by stretched exponentials at variance with the $\beta > 1$ behaviour found in previous studies[29–32] and in rejuvenated samples,[53] as fully discussed in ref. 53.
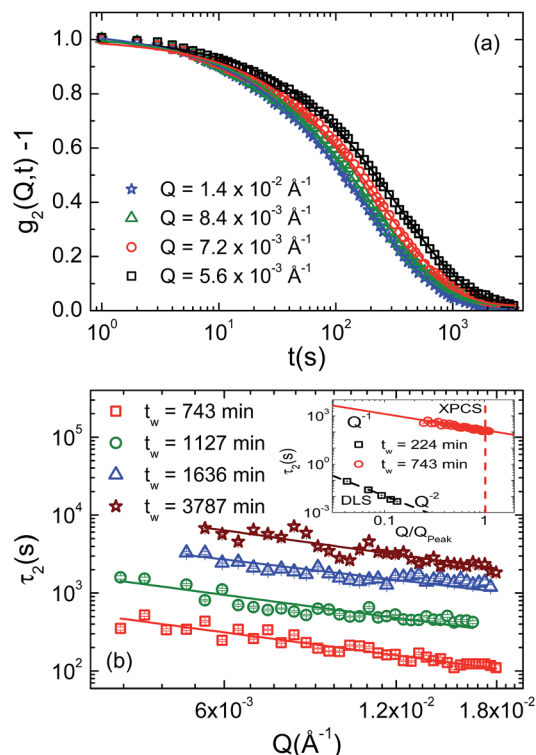
Fig. 3 (a) Normalized intensity correlation functions measured using XPCS for different Q-values at $t_w = 1127$ min. The solid lines are stretched exponential fits. (b) Q-dependence of the slow relaxation time at different waiting times. The solid lines are power law fits of the data as $\sim Q^{-n}$ where $n = 0.95 \pm 0.12$. Inset: comparison between slow relaxation times measured using DLS ($t_w = 9$ min) and XPCS ($t_w = 743$ min) as a function of Q/Q_{peak}. The dashed and full lines indicate respectively the Q^{-2} and Q^{-1} behaviours. The red vertical line indicates the position of the structure factor peak.
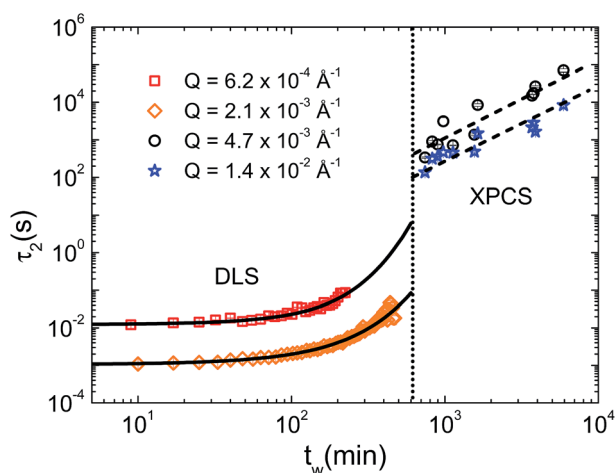

Fig. 4 Structural relaxation time as a function of waiting time measured using DLS and XPCS at different Q values. The full and dashed lines are the best fits to the data with exponentials and power laws respectively at small and large t_w. The vertical dotted line represents the sol-Wigner glass transition at $t_w \approx 600$ min.
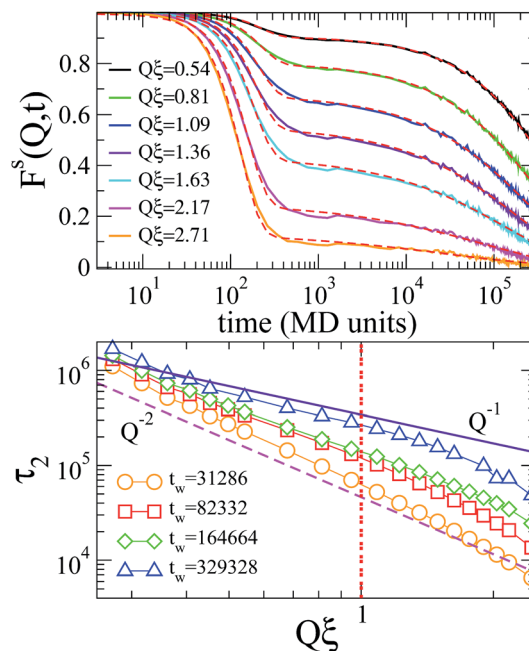

Fig. 5 (a) Self intermediate scattering functions (full lines) from MD simulations following a quench to $T = 1.6 \times 10^{-5}$ at fixed waiting time $t_w = 329\,328$ MD units and different wave vectors, as reported in the labels. The dashed lines are the fitting curves obtained using the expression within the square brackets of eqn (1) with $\gamma = 2$. (b) Q-dependence of the slow relaxation time τ_2 extracted from the fits for selected values of t_w. The dashed and full lines indicate respectively the Q^{-2} and Q^{-1} behaviours. The red vertical line indicates the position of the structure factor peak.

The combination of three complementary experimental techniques has allowed us to show that the fast relaxation mode remains diffusive both in ergodic and non-ergodic conditions at all waiting times. On the other hand, we observe that the structural relaxation time is characterized by two distinct Q behaviours in the two different t_w regimes. This crossover could be then interpreted by a change from diffusive dynamics to discontinuous hopping of caged particles, as predicted in ref. 25 by lowering the temperature in a glass forming system. It remains to elucidate what happens in between the DLS and XPCS regimes, *i.e.* whether the change is discontinuous or not. Bhattacharyya *et al.*[25] predicted a gradual change of the dynamics. To address this point we turn to MD simulations.

In Fig. 5(a) we report the MD self intermediate scattering functions (full lines) at a fixed waiting time after a quench in the glassy state for several wavevectors. The microscopic dynamics is Newtonian, thereby the data are fitted by the double exponential decay within the square brackets of eqn (1) fixing $\gamma = 2$ and the corresponding τ_1 is not relevant to describe the experimental (Brownian) fast relaxation. We discuss only wavevectors small enough that the second exponential in eqn (1) is stretched ($\beta < 1$), excluding large Q values where the dynamics becomes again ballistic due to the underlying microscopic dynamics.[54] In the early aging regime, the correlators do not display the typical two-step decay, similar to what was observed in out-of-equilibrium simulations of other glass formers.[55] We thus focus on the regime

occurring at larger waiting times, *i.e.* $t_w \gtrsim 20\,000$, where full aging starts and the double exponential describes the correlators, as shown by the fits in Fig. 5(a) (dashed lines). The corresponding τ_2 is reported as a function of Q in Fig. 5(b) for different values of the waiting time. We find that τ_2 initially displays Q^{-2} dependence at low and intermediate wave-vectors, in agreement with the DLS data of Fig. 1. Upon increasing t_w, while at low Q (approaching the hydrodynamic regime) τ_2 still tends to recover a diffusive behaviour (Q^{-2}), at intermediate Q encompassing the main structure factor peak (see the vertical line in Fig. 5(b)) a clear power-law dependence Q^{-n} with the exponent lowering and approaching unity at large t_w, is observed. At even larger t_w the system becomes non-ergodic on the timescale of our simulations. Thus, in the full aging regime we observe a strongly non-diffusive dependence of τ_2, approaching a Q^{-1} behaviour, in full agreement with the XPCS data in the same Q-window. Interestingly, n decreases continuously with increasing t_w in agreement with theoretical predictions.[25]

4   Conclusions

In this study we have investigated the Q-dependence of both microscopic and structural relaxation times during the early aging and full aging regimes of a colloidal glass using multi-angle DLS, NSE and XPCS techniques, covering a wide range of wavevectors and times. The experimental results have been complemented by MD simulations. We found that the microscopic relaxation time, τ_1, characteristic of the short-time diffusion of a particle in the suspending medium, scales as Q^{-2} during both early aging and full aging regimes, depicting a diffusive nature of particle motion. In contrast the slow relaxation time, τ_2, associated with the structural rearrangement of the system, shows a transition from a Q^{-2} diffusive behaviour in the liquid (or early aging) regime to a Q^{-1} activated dynamics in the glass (or full aging) regime associated with a stretched behaviour of the correlation functions, in full agreement with recent theoretical predictions.[25] Moreover this crossover is also associated with a dual waiting time dependence of τ_2: $\tau_2(t_w) \propto e^{t_w}$ in the early aging regime and $\tau_2(t_w) \propto t_w^{\alpha}$ in the full aging regime. Despite the peculiar and complex nature of Laponite,[45] the reported experimental evidence is not specific to the studied system. Indeed, our results confirm and extend previous detections of non-diffusive/activated dynamics in the supercooled regime reported both for molecular liquids, such as water[22] and *ortho*-terphenyl,[23] and for colloidal hard spheres.[24] Thus, our study of both relaxations in a colloidal glass-former should be considered as generic and be used as a reference for the description of the complex dynamics at fast and slow timescales of any glass-former.

Acknowledgements

References

1 P. G. Debenedetti and F. H. Stillinger, *Nature*, 2001, **410**, 259.
2 U. Balucani and M. Zoppi, *Dynamics of the Liquid State*, Clarendon Press - Oxford, 1994.
3 T. Scopigno, U. Balucani, G. Ruocco and F. Sette, *Phys. Rev. Lett.*, 2000, **85**, 4076.
4 R. Angelini, P. Giura, G. Monaco, G. Ruocco, F. Sette and R. Verbeni, *Phys. Rev. Lett.*, 2002, **88**, 255503.
5 G. Monaco, A. Cunsolo, G. Ruocco and F. Sette, *Phys. Rev. E: Stat. Phys., Plasmas, Fluids, Relat. Interdiscip. Top.*, 1999, **60**, 5505.
6 F. Mezei, W. Knaak and B. Farago, *Phys. Rev. Lett.*, 1987, **58**, 571.
7 D. L. Sidebottom, R. Bergman, L. Borjesson and L. M. Torell, *Phys. Rev. Lett.*, 1993, **71**, 2260.
8 M. Zuriaga, L. C. Pardo, P. Lunkenheimer, J. L. Tamarit, N. Veglio, M. Barrio, F. J. Bermejo and A. Loidl, *Phys. Rev. Lett.*, 2009, **103**, 075701.
9 S. Z. Ren and C. M. Sorensen, *Phys. Rev. Lett.*, 1993, **70**, 1727.
10 W. van Megen and S. M. Underwood, *Phys. Rev. Lett.*, 1993, **70**, 2766.
11 B. Abou, D. Bonn and J. Meunier, *Phys. Rev. E: Stat., Nonlinear, Soft Matter Phys.*, 2001, **64**, 021510.
12 S. Biffi, R. Cerbino, F. Bomboi, E. Paraboschia, R. Asselta, F. Sciortino and T. Bellini, *Proc. Natl. Acad. Sci. U. S. A.*, 2013, **24**, 15633.
13 W. Götze, *Complex Dynamics of Glass-forming Liquids: a Mode-coupling Theory*, Oxford Science Publications - Oxford, 2008.
14 D. L. Sidebottom, B. V. Rodenburg and J. R. Changstrom, *Phys. Rev. B: Condens. Matter Mater. Phys.*, 2007, **75**, 132201.
15 F. Mezei and W. Knaak, *Phys. Scr.*, 1987, **T19**, 363.
16 A. Tolle, *Rep. Prog. Phys.*, 2001, **64**, 1473.
17 A. Arbe, J. Colmenero, F. Alvarez, M. Monkenbusch, D. Richter, B. Farago and B. Frick, *Phys. Rev. Lett.*, 2002, **89**, 245701.
18 B. Farago, A. Arbe, J. Colmenero, R. Faust, U. Buchenau and D. Richter, *Phys. Rev. E: Stat., Nonlinear, Soft Matter Phys.*, 2002, **65**, 051803.
19 J. Colmenero, F. Alvarez, Y. Khairy and A. Arbe, *J. Chem. Phys.*, 2013, **139**, 044906.
20 L. Angelani, R. DiLeonardo, G. Ruocco, A. Scala and F. Sciortino, *Phys. Rev. Lett.*, 2000, **85**, 5356.
21 K. Broderix, K. K. Bhattacharya, A. Cavagna, A. Zippelius and I. Giardina, *Phys. Rev. Lett.*, 2000, **85**, 5360.
22 F. Sciortino, P. Gallo, P. Tartaglia and S. H. Chen, *Phys. Rev. E: Stat. Phys., Plasmas, Fluids, Relat. Interdiscip. Top.*, 1996, **54**, 6331.
23 A. Rinaldi, F. Sciortino and P. Tartaglia, *Phys. Rev. E: Stat., Nonlinear, Soft Matter Phys.*, 2001, **63**, 061210.
24 E. J. Saltzman and K. S. Schweizer, *Phys. Rev. E: Stat., Nonlinear, Soft Matter Phys.*, 2006, **74**, 061501.
25 S. M. Bhattacharyya, B. Bagchi and P. G. Wolynes, *J. Chem. Phys.*, 2010, **132**, 104503.

26 D. Bonn, H. Tanaka, G. Wegdam, H. Kellay and J. Meunier, *Europhys. Lett.*, 1999, **45**, 52.

27 L. Cipelletti, S. Manley, R. C. Ball and D. A. Weitz, *Phys. Rev. Lett.*, 2000, **84**, 2275.

28 A. Duri, T. Autenrieth, L.-M. Stadler, O. Leupold, Y. Chushkin, G. Grubel and C. Gutt, *Phys. Rev. Lett.*, 2009, **102**, 145701.

29 M. Bellour, A. Knaebel, J. L. Harden, F. Lequeux and J. P. Munch, *Phys. Rev. E: Stat., Nonlinear, Soft Matter Phys.*, 2003, **67**, 031405.

30 R. Bandyopadhyay, D. Liang, H. Yardimci, D. A. Sessoms, M. A. Borthwick, S. G. J. Mochrie, J. L. Harden and R. L. Leheny, *Phys. Rev. Lett.*, 2004, **93**, 228302.

31 S. Kaloun, R. Skouri, M. Skouri, J. P. Munch and F. Schosseler, *Phys. Rev. E: Stat., Nonlinear, Soft Matter Phys.*, 2005, **72**, 011403.

32 F. Schosseler, S. Kaloun, M. Skouri and J. P. Munch, *Phys. Rev. E: Stat., Nonlinear, Soft Matter Phys.*, 2006, **73**, 021401.

33 B. Ruta, Y. Chushkin, G. Monaco, L. Cipelletti, E. Pineda, P. Bruna, V. M. Giordano and M. Gonzalez-Silveira, *Phys. Rev. Lett.*, 2012, **109**, 165701.

34 P. Falus, M. A. Borthwick, S. Narayanan, A. R. Sandy and S. G. J. Mochrie, *Phys. Rev. Lett.*, 2006, **97**, 066102.

35 S. Narayanan, D. R. Lee, A. Hagman, X. Li and J. Wang, *Phys. Rev. Lett.*, 2007, **98**, 185506.

36 H. Guo, G. Bourret, M. K. Corbierre, S. Rucareanu, R. B. Lennox, K. Laaziri, L. Piche, M. Sutton, J. L. Harden and R. L. Leheny, *Phys. Rev. Lett.*, 2009, **102**, 075702.

37 C. Caronna, Y. Chushkin, A. Madsen and A. Cupane, *Phys. Rev. Lett.*, 2008, **100**, 055702.

38 J.-P. Bouchaud and E. Pitard, *Eur. Phys. J. E*, 2001, **6**, 231.

39 A. Mourchid, E. Lecolier, H. Van Damme and P. Levitz, *Langmuir*, 1998, **14**, 4718.

40 P. Mongondry, J. F. Tassin and T. Nicolai, *J. Colloid Interface Sci.*, 2005, **283**, 397.

41 H. Tanaka, S. Jabbari-Farouji, J. Meunier and D. Bonn, *Phys. Rev. E: Stat., Nonlinear, Soft Matter Phys.*, 2005, **71**, 021402.

42 S. Jabbari-Farouji, G. H. Wegdam and D. Bonn, *Phys. Rev. Lett.*, 2007, **99**, 065701.

43 H. Z. Cummins, *J. Non-Cryst. Solids*, 2007, **353**, 3892.

44 A. Shahin and Y. M. Joshi, *Langmuir*, 2010, **26**, 4219.

45 B. Ruzicka and E. Zaccarelli, *Soft Matter*, 2011, **7**, 1268; B. Ruzicka, E. Zaccarelli, L. Zulian, R. Angelini, M. Sztucki, A. Moussaïd, T. Narayanan and F. Sciortino, *Nature Materials*, 2011, **10**, 56–60.

46 V. Tudisca, M. Ricci, R. Angelini and B. Ruzicka, *RSC Adv.*, 2012, **2**, 11111.

47 B. Ruzicka, L. Zulian, E. Zaccarelli, R. Angelini, M. Sztucki, A. Moussaïd and G. Ruocco, *Phys. Rev. Lett.*, 2010, **104**, 085701.

48 C. Beck, W. Härtl and R. Hempelmann, *J. Chem. Phys.*, 1999, **111**, 8209.

49 E. Zaccarelli, S. Andreev, F. Sciortino and D. R. Reichman, *Phys. Rev. Lett.*, 2008, **100**, 195701.

50 H. Kang, T. R. Kirkpatrick and D. Thirumalai, *Phys. Rev. E: Stat., Nonlinear, Soft Matter Phys.*, 2013, **88**, 042308.

51 A. Madsen, R. Leheny, H. Guo, M. Sprung and O. Czakkel, *New J. Phys.*, 2010, **12**, 055001.

52 B. Ruzicka, L. Zulian and G. Ruocco, *Phys. Rev. Lett.*, 2004, **93**, 258301.

53 R. Angelini, L. Zulian, A. Fluerasu, A. Madsen, G. Ruocco and B. Ruzicka, *Soft Matter*, 2013, **9**, 10955; R. Angelini, E. Zaccarelli, F. A. de Melo Marques, M. Sztucki, A. Fluerasu, G. Ruocco and B. Ruzicka, *Nature Communications*, 2014, **5**, 1049.

54 S. Saw, N. L. Ellegaard, W. Kob and S. Sastry, *Phys. Rev. Lett.*, 2009, **103**, 248305.

55 D. El Masri, L. Berthier and L. Cipelletti, *Phys. Rev. E: Stat., Nonlinear, Soft Matter Phys.*, 2010, **82**, 031503.